

Comparative Study of Two Oxy-Fuel Power Systems with LNG (Liquefied Natural Gas) Cryogenic Energy Utilization

Na Zhang^{*1}, Meng Liu¹, Noam Lior², Wei Han¹

¹Institute of Engineering Thermophysics, Chinese Academy of Sciences
Beijing 100080, P. R. China

²Department of Mechanical Engineering and Applied Mechanics
University of Pennsylvania
Philadelphia, PA 19104-6315, USA

ABSTRACT: A novel liquefied natural gas (LNG) fueled power plant is proposed, which has virtually zero CO₂ and other emissions and a high efficiency. The plant operates as a subcritical CO₂ Rankine-like cycle. Beside the power generation, the system provides refrigeration in the CO₂ subcritical evaporation process, thus it is a cogeneration system with two valued products, three if credit is given for the liquefied CO₂. By coupling with the LNG evaporation system as the cycle cold sink, the cycle condensation process can be achieved at a temperature much lower than ambient, and high-pressure liquid CO₂ can be withdrawn from the cycle without consuming additional power. Two system variants are analyzed and compared, OXYF and OXYF-COMP. In the OXYF cycle configuration, the working fluid in the main turbine expands only to the CO₂ condensation pressure, the advantage is that the backwork is very small since the low pressure fluid is in liquid phase and can thus be pumped (rather than compressed) to the higher pressure. In the OXYF-COMP cycle configuration, the turbine working fluid expands to a much lower pressure (near-ambient) to produce more power. However, it then requires a compressor to raise the CO₂ pressure to the condensation level. The two system configurations are compared with and without turbine blade cooling. The effects of some key parameters, the turbine inlet temperature *TIT* and the backpressure, on the systems' performance are investigated. It is found that without turbine blade cooling, at the turbine inlet temperature of 900°C, the energy efficiency of the OXYF system reaches 59%, which is higher than the 52% of the OXYF-COMP one. The capital investment cost of the economically optimized plant is about \$1,000/kWe and the payback period is about 8-10.5 years including the construction period, both better than those of the latest conventional fossil fuel power plants built in China that do not even separate the CO₂, and the cost of electricity is estimated to be 0.34-0.37 CNY/kWh.

Keywords: Oxy-Fuel power system, LNG, cryogenic energy, power generation

* Corresponding author: Phone: +86 10 82543030 Fax: +86 10 62575913 E-mail: zhangna@mail.etp.ac.cn

Nomenclature

| | |
|-----------------|--|
| A | Area [m ²] |
| C_{CO_2} | The annual CO ₂ credit (10 ⁶ CNY) |
| C_f | The annual fuel cost (10 ⁶ CNY) |
| C_i | The total plant investment (10 ⁶ CNY) |
| C_m | The annual the O&M cost (10 ⁶ CNY) |
| C_p | Specific heat [kJ/kg·k] |
| COE | Cost of electricity [CNY/kWh] |
| e | Specific exergy [kJ/kg]; Film cooling effectiveness |
| E_c | Total refrigeration exergy output [MW] |
| H | The annual operation hours [h] |
| LHV | Lower heating value of fuel [kJ/kg] |
| m | Mass flow rate [kg/s] |
| n | The plant operation life [year] |
| p | Pressure [bar] |
| p_b | Backpressure [bar] |
| Q | Heat [kW] |
| Q_c | Refrigeration [kW] |
| R | Ratio of net power output to refrigeration exergy |
| R_{CO_2} | CO ₂ recovery ratio |
| s | Specific entropy [kJ/kg·K] |
| St | Stanton number |
| T | Temperature [°C] |
| TIT | Turbine inlet temperature [°C] |
| TOT | Turbine outlet temperature [°C] |
| W_{net} | Net power output (after deducting also the ASU power consumption) [MW] |
| w | Specific power output [kJ/kg] |
| η_c | Blade cooling efficiency [%] |
| β | Coefficient, Eq. (5) |
| η_e | Power generation efficiency [%], Eq. (1) |
| ε | Exergy efficiency [%], Eq. (2) |
| ε_c | Cooling effectiveness |
| Subscripts | |
| b | Blade |
| c | Cooling, coolant |
| f | Fuel |

| | |
|---------------|--------------------------------|
| g | Gas |
| LNG | LNG |
| wf | Working fluid |
| 1,2...23 | States on the cycle flow sheet |
| Abbreviations | |
| ASU | Air separated Unit |
| BOP | Balance of plant |
| C | Compressor |
| CNY | Chinese Yuan |
| COM | Combustor |
| CON | Condenser |
| EVA | Evaporator |
| HEX | Heat exchanger |
| LHV | Fuel lower heating value |
| LNG | Liquid natural gas |
| NG | Natural gas |
| REP | REcuperator |

1. INTRODUCTION

Liquefied natural gas (LNG) is used widely, and approximately 500 kWh energy per ton LNG is consumed for its compression and refrigeration during the process of its preparation from the original low-pressure gaseous form, to reduce its volume (about 600-fold) for much easier storage and long distance transportation. An important aspect is that a considerable portion of this invested energy and exergy are preserved in the LNG [1], which has a final temperature of about 110K, much lower than that of the ambient air or water.

At the receiving terminals, LNG is off-loaded and pumped, revaporized and heated to approximately ambient temperature for pipeline transmission to the consumers. Instead of simply providing the heat for this process from ambient seawater or air, as is often done in practice, and thus wasting the valuable coldness, it is possible to withdraw the cryogenic exergy from the LNG evaporation process by investing it in some process which recovers it for some useful application. One way to achieve this is by incorporating it into a properly designed thermal power cycle that

uses the LNG evaporator as its cold sink [1-13].

Use of the cryogenic exergy of LNG for power generation includes methods which use the LNG as the working fluid in natural gas direct expansion cycles, or its coldness as the heat sink in closed-loop Rankine cycles [1-6], Brayton cycles [7-9], and combinations thereof [10, 11]. Other methods use the LNG coldness to improve the performance of conventional thermal power cycles. For example, LNG vaporization can be integrated with gas turbine inlet air cooling [5, 12] or steam turbine condenser system (by cooling the recycled water [11]), etc. Some pilot plants have been established in Japan from the 1970's, combining closed-loop Rankine cycles (with pure or mixture organic working fluids) and direct expansion cycles [1].

Increasing concern about greenhouse effects on climatic change prompted a significant growth in research and practice of CO₂ emission mitigation in recent years. The main technologies available for CO₂ capture in power plants are physical and chemical absorption, cryogenic fractionation, and membrane separation. The amount of energy needed for the CO₂ capture would lead to the reduction of power generation energy efficiency by up to 10 percentage points [14, 15].

Beside the efforts for reduction of CO₂ emissions from existing power plants, concepts of power plants having zero CO₂ emission were proposed and studied. Oxy-fuel combustion is one of the proposed removal strategies. It is based on the close-to-stoichiometric combustion, where the fuel is burned with enriched oxygen (produced in an air separation unit ASU) and recycled flue gas. The combustion is accomplished in absence of the large amounts of nitrogen and produces only CO₂ and H₂O. CO₂ separation is accomplished by condensing water from the flue gas and therefore requires only a modest amount of energy. Some oxy-fuel cycles with ASU and

recycled CO₂/H₂O from the flue gas are the Graz cycle, Water cycle and Matiant cycle [16-20]. We proposed and analyzed the semi-closed oxy-fuel cycles with integration of the LNG cold exergy utilization [21, 22]. The additional power use for O₂ production amounts to 7~10% of the cycle total input energy. To reduce the oxygen production efficiency penalty, new technologies have been developed, such as chemical looping combustion (CLC)^[23, 24] and the AZEP concept^[25], employing oxygen transport particles and membranes to separate O₂ from air. Kvamsdal et al [26] made a quantitative comparison of various cycles with respect to plant efficiency and CO₂ emissions, concluded that the adoption of these new technologies shows promising performance because no additional energy is then necessary for oxygen separation, but they are still under development.

In this paper we present, model, and compare two novel power generation systems with LNG cold energy and CO₂ capture. The first system concept, here named OXYF, is based on the concept proposed by Deng et al [6]: that is a cogeneration (power and refrigeration) recuperative Rankine cycle with CO₂ as the main working fluid. Combustion takes place with natural gas burning in an oxygen and recycled-CO₂ mixture. The high turbine inlet temperature and turbine exhaust heat recuperation present a high heat addition temperature level, and the heat sink at a temperature lower than the ambient accomplished by heat exchange with LNG offer high power generation efficiency. At the same time, these low temperatures allow condensation of the working fluid and the combustion generated CO₂ is thus captured. Furthermore, the sub-critical re-evaporation of the CO₂ working fluid is accomplished below ambient temperature and can thus provide refrigeration if needed.

Our second system concept, here named the OXYF-COMP cycle is a variation of the OXYF cycle but with a lower turbine backpressure to generate a higher power

output. These systems have both high power generation efficiency and extremely low environmental impact.

The primary advances over the work presented in [6] are the integration of the LNG evaporation with the CO₂ condensation and capture. In the analysis in [6], it was assumed that LNG consists of pure CH₄ and the combustion production after water removal can be fully condensed at the 5.3bar/-53.1°C. In this paper we proposed and analyzed a system with a different condensation process: first the amount of the working fluid needed for sustaining the process is condensed and recycled, and the remaining working fluid, having a relatively small mass flow rate (<5% of the total turbine exhaust flow rate after water removal) and higher concentration of noncondensable gases, are compressed to a higher pressure level and then condensed. Alternatively, the CO₂-enriched flue gas can be condensed at a lower temperature, which can be provided

by the LNG coldness, but it would then freeze the CO₂ and is thus not considered in this paper; instead we adopted a higher condensation pressure for the flue stream condensation, which leads to a more conservative solution and some efficiency penalty but can recover the CO₂ fully. Another advancement relative to [6] is that here we also consider the need and effects of turbine blade cooling on the process, while in [6] a *TIT* of 1250 °C without blade cooling was assumed, which is too high for practical systems and leads to a more optimistic system performance prediction.

2. SYSTEM CONFIGURATION DESCRIPTION

The two system configurations proposed and analyzed generate power and produce refrigeration if needed, evaporate LNG (and thus convert the LNG cold for power generation), and capture the combustion generated CO₂. They are:

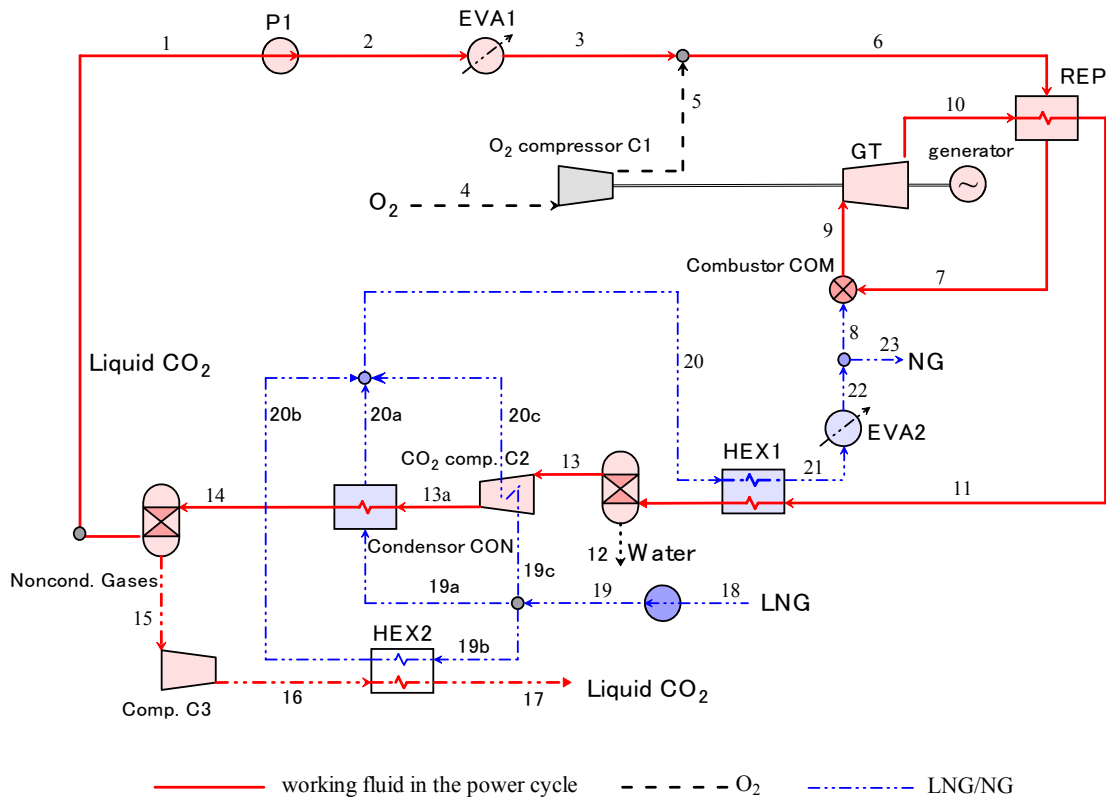


Fig. 1 The process flowsheet of the OXYF-COMP system

- OXYF, in which the working fluid in the main turbine expands only to the CO₂ condensation pressure.
- OXYF-COMP, in which the turbine working fluid expands to a much lower pressure (near-ambient) to produce more power. In addition, the turbine exhaust temperature, and therefore the regenerator hot stream inlet temperature are at a lower level, eliminating the need for the higher temperature heat exchanger. However, it then requires a compressor to raise the CO₂ pressure to the condensation level.

2.1 The OXYF-COMP configuration

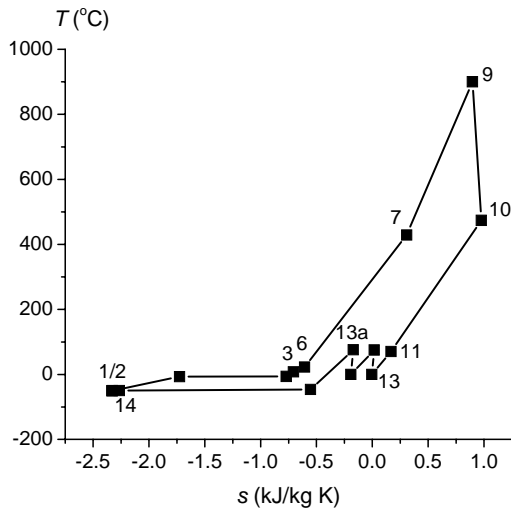


Fig.2 Cycle T - s diagram in the OXYF-COMP system

Figure 1 shows the layout of the OXYF-COMP cycle, which consists of a power subcycle and an LNG vaporization process. Fig. 2 is the cycle T - s diagram. The interfaces between the power subcycle and the LNG vaporization process are the CO₂ condenser CON, the heat exchangers HEX1, and the fuel feed stream 8.

The power subcycle can be identified as 1-2-3-4-5-6-7-8-9-10-11-12/13-13a-14-1. The low temperature (-50°C) liquid CO₂ as the main working fluid (1) is pumped to about 30 bar (2), then goes through a heat addition process (2-3) in the evaporator

EVA1 and can thereby produce refrigeration if needed. The O₂ (4) produced in an air separator unit (ASU) is compressed and mixed with the main CO₂ working fluid. The gas mixture (6) is heated (6-7) by turbine (GT) exhaust heat recuperation in REP. The working fluid temperature is further elevated in the combustor COM, fueled with natural gas (8), to its maximal value (the turbine inlet temperature TIT) (9). The working fluid expands to near-ambient pressure (10) in the gas turbine (GT) to generate power and is then cooled (to 11) in the recuperator REP.

The gases in the mixture at the exit of REP (11) need to be separated, and the combustion generated CO₂ component needs to be condensed for ultimate sequestration, and this is performed by further cooling: in the LNG-cooled heat exchanger HEX1, in which the H₂O vapor in the mixture is condensed and drained out (12). Afterwards, the remaining working gas (13) is compressed to the condensation pressure, and one stage inter-cooling (19c-20c) is adopted in the compressor to reduce the compression work. The CO₂ working fluid is condensed (13b) in the condenser CON against the LNG evaporation, and recycled (1). The remaining working fluid (15) enriched with noncondensable species (mainly N₂) is further compressed in C3 to a higher pressure level under which the combustion-generated CO₂ is condensed and captured, ready for final disposal.

The LNG vaporization process is 18-19-19a/b/c-20a/b/c-20-21-22-23/8. LNG (18) is pumped by P_2 to the highest pressure (73.5bar), typical for receiving terminals which supply long distance pipeline network, and then evaporated with the heat addition from the power cycle. The evaporated NG (natural gas) may produce a small amount of cooling in HEX3 if its temperature is still low enough at the exit of HEX1, and thus contribute to the overall system useful outputs. Finally, the emerging natural gas stream is split into two parts where most of it (23) is sent to outside users and a small part (8) is used as the fuel in the combustor

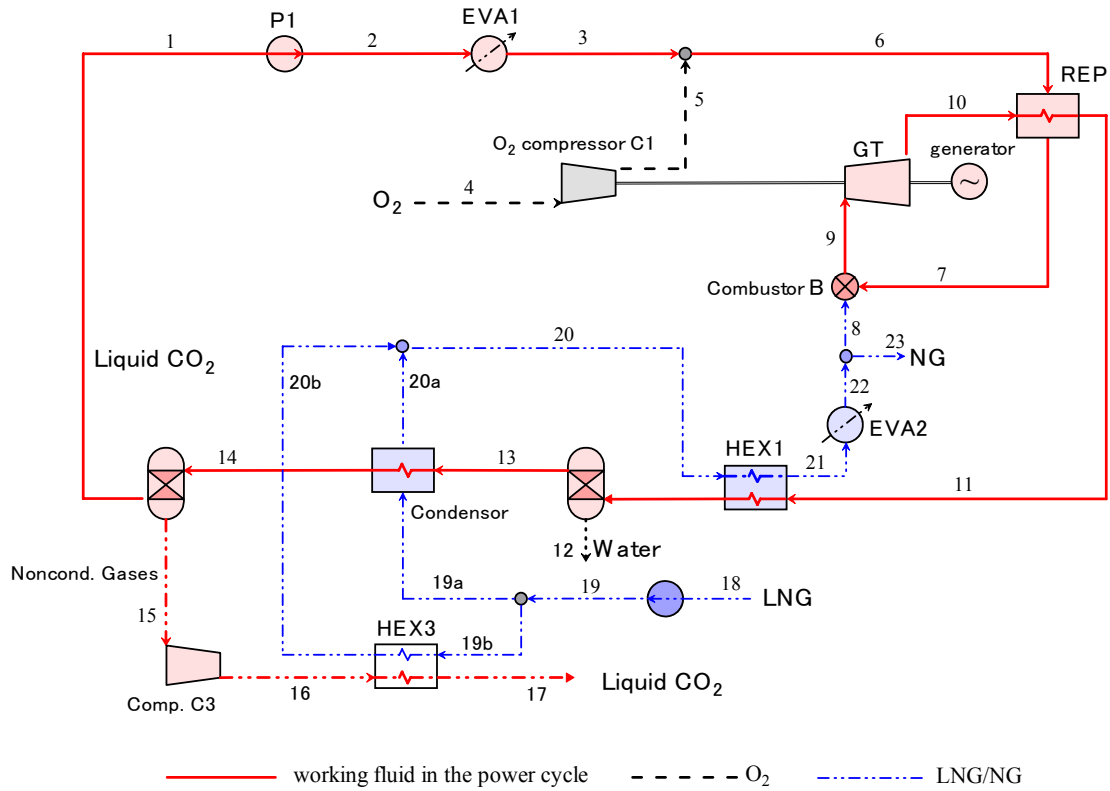


Fig. 3 The process flowsheet of the OXYF system

of this cycle.

In this configuration, a compressor C2 is required to raise the expanded CO₂ gas pressure to the condensation level, with the associated efficiency penalty due to the energy consumption of the compressor.

2.2. The OXYF configuration

Noting from preliminary analysis that the necessity for the gas compressor in system OXYF-COMP (process 13-13a in Figs. 1 and 2) consumes a significant amount of power for the pressure elevation, system OXYF was configured so that the working fluid expands in the turbine GT to only the working fluid condensation pressure, at the expense of some amount of power generation in the turbine, thus eliminating the need for this gas compression process. The working fluid pressure elevation is accomplished entirely by the much less energy consuming process of pressurizing a liquid (process 1-2 in Fig. 3).

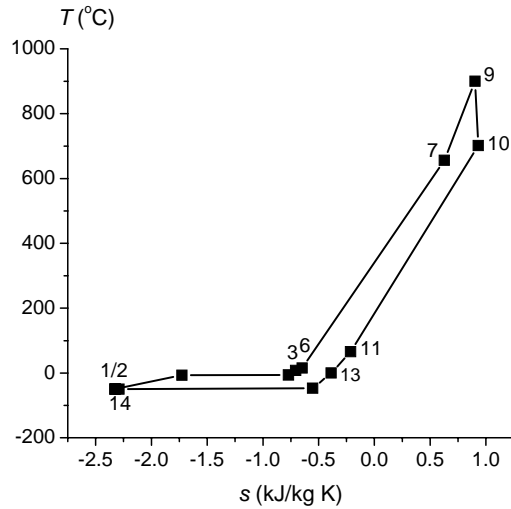


Fig.4 Cycle T-s diagram in the OXYF system

Fig. 4 is the cycle T - s diagram. In comparison with OXYF-COMP, system OXYF eliminates the CO₂ compressor C2 from the cycle configuration. As a result, the turbine in OXYF has a higher back pressure compared with that in OXYF-COMP and its exhaust is at a higher temperature (the

regenerator REP hot stream inlet temperature), and, as shown in Section 4 below, its energy efficiency is superior to that of OXYF-COMP. It is noted that the higher temperature in heat exchanger REP requires special attention to its design.

3. CALCULATION ASSUMPTIONS

The simulations were carried out using the commercial Aspen Plus software [27], in which the component models are based on the energy balance and mass balance, with the default relative convergence error tolerance of 0.01%. The PSRK property method was selected for the thermal property calculations. It is based on the Predictive Soave-Redlich-Kwong equation-of-state model, which is an extension of the Redlich-Kwong-Soave equation of state. It can be used for mixtures of non-polar and polar compounds, in combination with light gases, and up to high temperatures and pressures. Some properties of feed streams are reported in Table 1, and the main assumptions for simulations are summarized in Table 2.

95 mol% oxygen from a cryogenic ASU is chosen for the combustion, since this was

considered to be the optimal oxygen purity when taking into account the tradeoff between the cost of producing the higher-purity oxygen and the cost of removing non-condensable species from the CO₂. The O₂ composition and its power consumption for production follow those in [26]. Some other assumptions for the calculation are summarized in Table 2.

Table 1. Molar composition and some properties for feed streams

| | LNG | O ₂ |
|---|--------|----------------|
| CH ₄ [mol %] | 90.82 | |
| C ₂ H ₆ [mol %] | 4.97 | |
| C ₃ H ₈ [mol %] | 2.93 | |
| C ₄ H ₁₀ | 1.01 | |
| N ₂ [mol %] | 0.27 | 2 |
| O ₂ [mol %] | | 95 |
| CO ₂ [mol %] | | |
| H ₂ O [mol %] | | |
| Ar [mol %] | | 3 |
| Temperature [°C] | -161.5 | 25 |
| Pressure [bar] | 1.013 | 2.38 |
| Lower heating value [kJ/kg] | 49200 | - |
| Power consumption for O ₂ production [kJ/kg] | | 812 |

Table 2. Main assumptions for the calculation of the systems

| | | |
|---|--|-------|
| Ambient state | Temperature [°C] | 25 |
| | Pressure [bar] | 1.013 |
| Combustor | Pressure loss [%] | 3 |
| | Efficiency [%] | 100 |
| | ExcessO ₂ beyond the stoichiometric ratio [%] | 2 |
| Gas turbine | Isentropic efficiency [%] | 90 |
| Recuperator | pressure loss [%] | 3 |
| | Minimal temperature difference [°C] | 45 |
| LNG vaporization unit | Pressure loss [%] | 2~3 |
| | Temperature difference at pinch point [°C] | 8 |
| CO ₂ condenser | Condensation pressure [bar] | 7 |
| | Condensation temperature [°C] | -50 |
| Pump efficiency [%] | | 80 |
| Compressor efficiency [%] | | 88 |
| (Mechanical efficiency) x (generator electrical efficiency) [%] | | 96 |

generation efficiency is defined as:

The commonly used thermal power

$$\eta_e = W_{net} / (m_f \cdot LHV) \quad (1)$$

Since the power and refrigeration cogeneration energy efficiency definition is problematic (cf. [28]), for evaluating the cogeneration we use the exergy efficiency as:

$$\varepsilon = (W_{net} + E_c) / (m_f \cdot e_f + m_{LNG} \cdot e_{LNG}) \quad (2)$$

with both the power and cooling as the outputs, and both the fuel exergy and LNG cold exergy as the inputs. The cooling rate exergy E_c is the sum of the refrigeration exergy produced in the evaporators EVA1 and EVA2. In the calculation below, the processed LNG mass flow rate is chosen to be the least which can sustain the cooling demand of the power cycle exothermic process.

The CO₂ recovery ratio R_{CO_2} is defined as:

$$R_{CO_2} = m_{R,CO_2} / m_{COM,CO_2} \quad (3)$$

where m_{COM,CO_2} is the combustion generated CO₂, and m_{R,CO_2} is the mass flow rate of the liquid CO₂ (17) that is retrieved.

The turbine inlet temperature TIT is a key parameter for the system performance, generally the higher the TIT , the higher the system efficiency. However, higher turbine inlet temperature always requires advanced combustor and turbine blade design and cooling, and also advanced materials, and will thus lead to the increase of the gas turbine cost.

Blade cooling has also significant influence on the gas turbine performance because 1) extraction of the coolant gas from the working fluid decreases the working fluid mass flow rate for power generation; 2) its mixing with the main gas reduces the local gas temperature and pressure, leading to further loss of power generation; 3) in a recuperative gas turbine cycle, the gas turbine exhaust temperature decreases and less exhaust heat is therefore available for recuperation, leading to drop of the combustor working fluid inlet

temperature and consequently to a higher fuel demand. With the conventional blade cooling technology, such as the convective or film cooling, higher TIT requires a higher blade coolant flow extraction. As TIT is raised there is point at which the gain from the increase of TIT will be offset by these negative effects of blade coolant application. At TIT values higher than this, the gas turbine efficiency drops. In this study, we assume that the turbine inlet temperature is 900°C, regarded as the highest that still does not require turbine blades cooling. The performance with and without turbine cooling is compared below. A description of the turbine blade cooling model is given in the Appendix.

To avoid CO₂ freezing, the condensation pressure is kept above the triple point pressure of 5.18 bar, and the temperature is chosen to be above -50°C. As mentioned before, we therefore chose a higher condensation pressure rather than a lower temperature. The simulation has shown that at the condensation pressure of 7 bar, the mass flow rate of the condensed CO₂ is merely sufficient for the working fluid recycling; and that the condensed CO₂ flow rate increases as the condensation pressure increases. The higher condensation pressure, however, requires more compressor work, resulting in lower system efficiency. Considering the significant influence of the condensation pressure on both system thermal performance and the CO₂ recovery, the working fluid is compressed to 7 bar, and then the CO₂ is condensed for recycling as the working fluid. Only the remaining uncondensed working fluid that has a mass flow rate of only 2%~5% of the total turbine exhaust after water removal, and high concentration of noncondensable species (the composition is about 88 mole % CO₂, and ~12 mole % of the noncondensable gases N₂, O₂ and Ar) will thus be compressed to a higher pressure for the CO₂ condensation and recovery. In this way, most of the working fluid is compressed to 7 bar, and only a small fraction of the working

fluid needs to be compressed to a higher pressure.

As mentioned before, the major difference between the two configurations is the turbine backpressure. In both systems, the CO₂ condensation pressures are the same at 7 bar, but the turbine exhaust pressures are different: 1.1 bar in the OXYF-COMP system and 7.1 bar in the OXYF system. In the OXYF-COMP system, a CO₂ compressor is incorporated to elevate the working fluid pressure for CO₂ condensation. To take advantage of the LNG coldness and to reduce the compressor power consumption, the compressor inlet stream should be cooled to a possibly lower temperature. However, to eliminate the technological difficulty associated with the low inlet temperature compressor, in this study the turbine exhaust gas is cooled in HEX1 just to 0°C. Water is condensed and removed before CO₂ compression in C₂. A trace amount of CO₂ will in any case be dissolved in the water and be removed along with it; to simplify the simulation it is assumed that water and CO₂ are fully separated.

A parametric analysis is conducted to investigate the influence of key parameters, which are the turbine inlet temperature and the turbine backpressure. Based on these analyses, the parameters are chosen and the two configurations are compared.

4. PARAMETRIC SENSITIVITY ANALYSIS

4.1. Investigation on the influence of the turbine inlet temperature TIT

We vary the TIT from 900°C to 1240°C and the two cases with or without gas turbine blade cooling are investigated and compared. The parameters examined are the specific power output w , the fuel mass flow m_f , the LNG mass flow m_{LNG} , the cycle thermal efficiency η_e and the cogeneration exergy efficiency ε . The parameters listed in Table 2 are kept constant in the sensitivity

analysis.

Figure 5 shows that the increasing the turbine inlet temperature TIT increases the specific power output w , as well as the extent to which turbine blade cooling reduces w . Obviously the blade cooling has bigger influence at higher TIT because of the higher demand of cooling stream extraction, and its effect is also higher in the OXYF system. The OXYF-COMP system has a much higher w than OXYF, because the turbine in the former expands to a much lower backpressure.

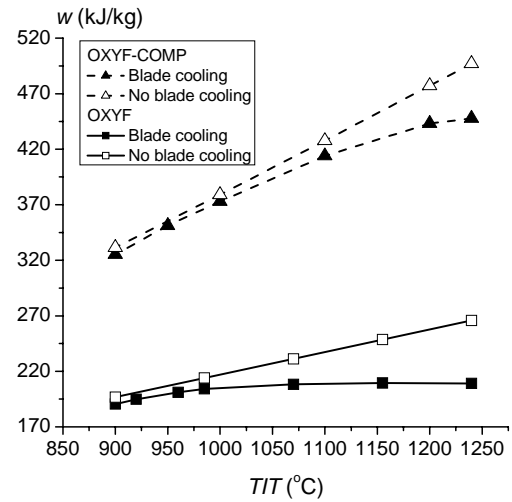


Fig.5 The specific power output w vs. TIT

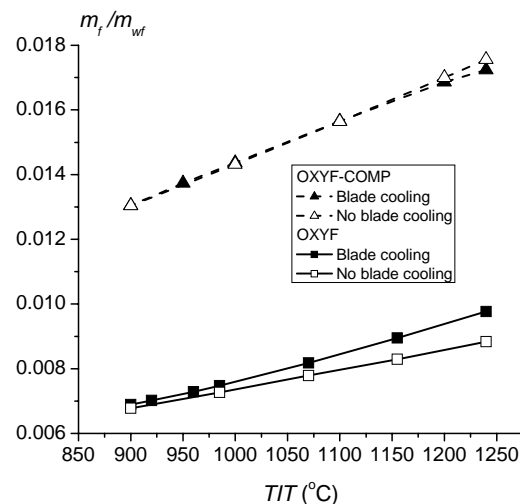


Fig.6 The fuel mass flow rate m_f vs. TIT

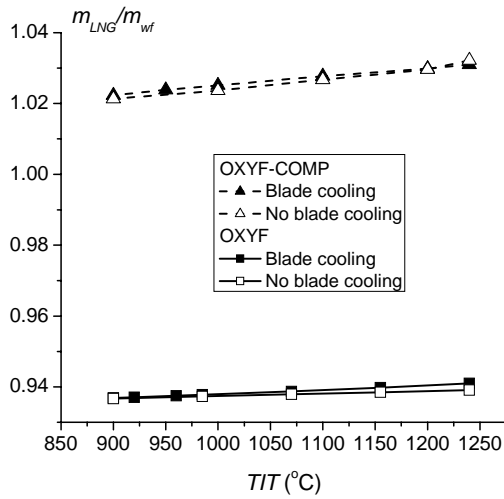


Fig. 7 The evaporated LNG mass flow rate vs. TIT

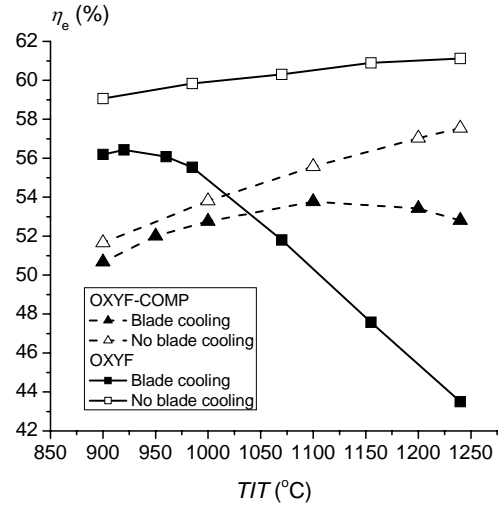


Fig. 8 The power generation efficiency η_e vs. TIT

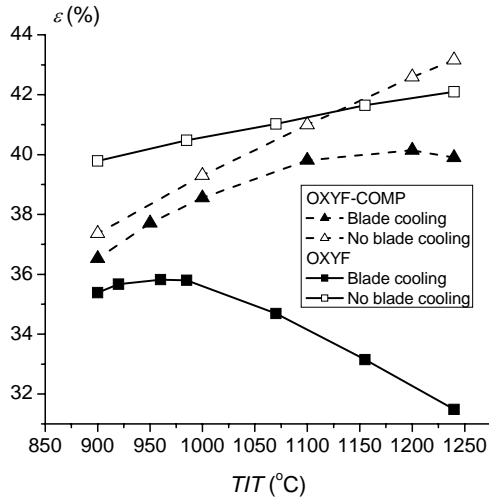


Fig. 9 The cogeneration exergy efficiency ε vs. TIT

Figure 6 shows the variation with TIT of the mass flow rate of the fuel used in the system combustor, normalized by the basic (i.e., the recycled) working fluid (stream 1 in Figs. 1 and 3). Increasing the TIT requires more fuel. For the same TIT , the fuel consumption is double in the OXYF-COMP than that in the OXYF system, because, the turbine exhausts at a much lower temperature in OXYF-COMP, making less heat available for recuperation and therefore creating a larger fuel demand elevating the working fluid temperature after the recuperation in REP.

Since the main ultimate use of an LNG terminal is to produce evaporated gas for consumption, we show in Fig. 7 the variation of the evaporated LNG mass flow rate, also normalized by the basic working fluid mass flow rate) with TIT . The LNG mass flow m_{LNG} is seen to slightly increase as TIT is increased. Blade cooling is seen to have a very small effect on the evaporated LNG flow rate.

The effect of TIT on the cycle power generation efficiency η is shown in Fig. 8. When blade cooling is used, the energy efficiency exhibits a maximum. For the OXYF-COMP cycle, the TIT at which the power generation efficiency has a maximum, of 53.8%, is about 1100 °C; and for the OXYF system the maximal power generation efficiency, of 56.4%, is at the much lower TIT of ~920 °C. At $TIT < 1040^\circ\text{C}$, the OXYF system has higher power generation efficiency than OXYF-COMP, but drops quickly below it as TIT increases. Without blade cooling, the power generation efficiency of OXYF exhibits a monotonic increase with increasing TIT , and is higher than that of the OXYF-COMP system, especially is the lower TIT region. For example, when $TIT=900^\circ\text{C}$ and without blade cooling, the power generation efficiency for OXYF is

59.1%, higher by 7.4%-points than that for OXYF-COMP.

The cogeneration exergy efficiency, which accounts for both power and cooling outputs, is shown in Fig. 9. It has similar variation tendency with TIT as there is also a value of TIT that maximize the efficiency when blade cooling is used. Without blade cooling, the OXYF system has better performance in the lower TIT region, the exergy efficiency ε is 39.8% for $TIT=900^\circ\text{C}$. The OXYF-COMP system has higher ε in the higher TIT region.

The conclusions from this analysis with and without turbine blade cooling is that the turbine blade cooling has a significant influence on the system performance especially in the high TIT region; for example for the OXYF system, the blade cooling causes a reduction of 4% - 9% of the specific power output w when $TIT < 1050^\circ\text{C}$, and its effect increases in the higher TIT region, and the efficiencies deteriorate too. It suggested that advanced cooling technology, such as transpiration, should be employed in the higher TIT region instead of the conventional convective and film cooling considered in this analysis. In our case, the higher TIT values are thus undesirable because they both reduce the efficiency and raise the turbine system cost.

Turbine blade cooling has bigger detrimental influence on the OXYF system

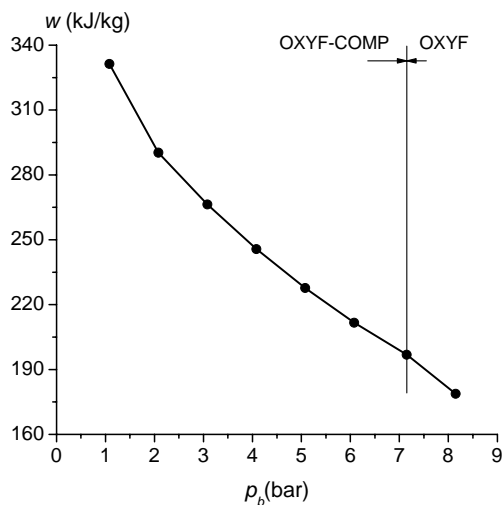


Fig. 10 The specific power output w vs. p_b

than on the OXYF-COMP. For the OXYF system, the power generation efficiency is 59.1% without blade cooling at 900°C (the highest limit for a gas turbine without blade cooling). Based on this analysis, we concluded that a turbine with a TIT of $\sim 900^\circ\text{C}$ and without blade cooling should be chosen to be investigated further. Reducing TIT from 1240°C to 900°C avoids the design and operation difficulty of the turbine, and makes it unnecessary to choose the most advance gas turbine with the associated higher capital and maintenance costs.

4.2 Investigation on the influence of turbine backpressure p_b

In the calculation below, the turbine inlet temperature TIT is fixed at 900°C and blade cooling is not employed. The calculation region can be divided into two:

- 1) for $P_b < 7.1$ bar, the system configuration is the OXYF-COMP, in which the CO_2 condensation pressure remains unchanged at 7 bar as P_b is varied from 1.1 bar to 7.1 bar.
- 2) for $P_b > 7.1$ bar, the CO_2 compression before condensation is not necessary any more, the system configuration is the OXYF, in which the CO_2 condensation pressure varies with the value of p_b .

Figure 10 shows the variation of the system specific power output with p_b . Though the increase of p_b reduces the power

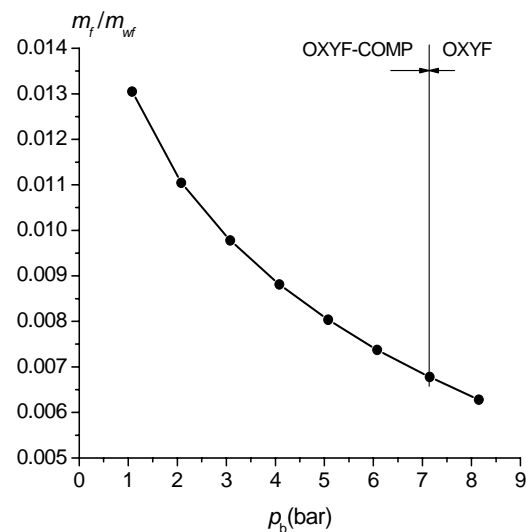


Fig. 11 The fuel mass flow rate m_f vs. p_b

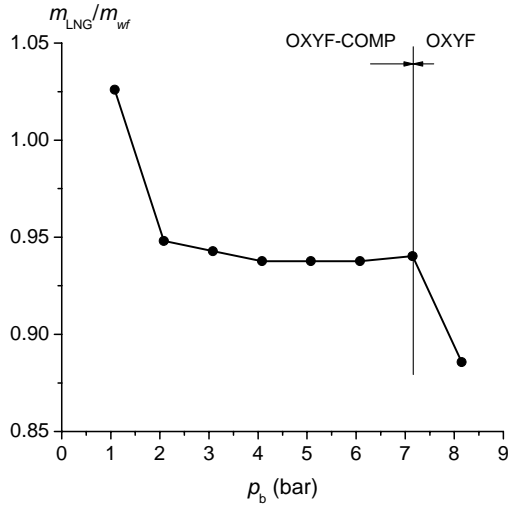


Fig. 12 The evaporated LNG flow rate m_{LNG} vs. p_b

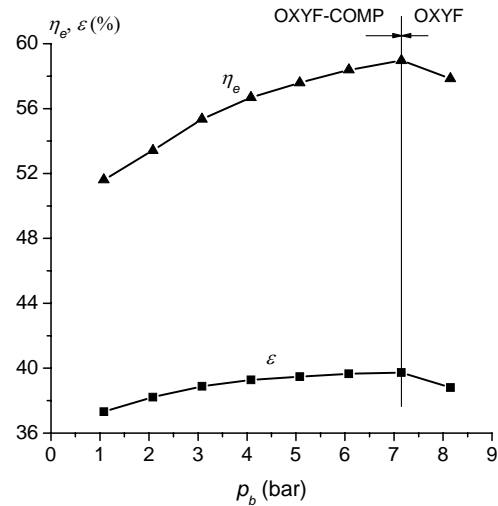


Fig. 13 The efficiencies η_e and ε vs. p_b

consumption of the CO₂ compressor C2, it has a more significantly negative effect on the turbine power output, leading to the drop of the net power output. In the investigated range, the highest specific power output of 330 kJ/kg is found for the OXYF-COMP system with p_b of 1.1 bar. For the OXYF-b system with the backpressure of 7.1 bar, the specific power output is about 197 kJ/kg. More importantly, this value is comparable or even higher than the specific power output of commercial gas turbines with the same TIT value of 900°C.

Figure 11 shows that raising p_b decreases the required fuel mass flow m_f . This is because the increasing turbine exit temperature that accompanies the increase of turbine backpressure makes more heat available for recuperation, thus reducing the fuel demand in the combustor.

Figure 12 shows that raising p_b decreases the mass flow of the LNG being evaporated by the system. As mention before, raising the backpressure makes more turbine exhaust heat available for recuperation, and therefore less heat available for LNG evaporation, indicated by the drop of the flue gas temperature at the exit of REP. In this calculation, the minimal temperature difference ΔT_P in the recuperator is fixed as 45°C at the hot end of REP.

Figure 13 shows the variation of the

power generation efficiency with p_b . For $p_b < 7.1$ bar, the system configuration is the OXYF-COMP. Raising p_b increases the thermal efficiency η_e from 51.6% (at $p_b=1.1$ bar) to 59% (at $p_b=7.1$ bar). This is mainly because of the drop of the fuel demand as show in Fig. 8. In the region $p_b \geq 7.1$ bar the system changes to the OXYF-b configuration, and increasing p_b beyond 7.1 bar decrease the efficiency. This is because both the turbine power generation and the fuel demand drop as the backpressure increases, but the drop of the turbine power output dominates in this case. The exergy efficiency ε undergoes a similar trend of rising from 37.3% (at $p_b = 1.1$ bar) to 39.7% (at $p_b = 7.1$ bar) and then decreasing for $p_b \geq 7.1$ bar.

The results suggest that although increase of the turbine backpressure p_b causes a decrease in the net power output, it raises the cycle thermal efficiency η_e and the exergy efficiency ε as long as p_b is lower than the CO₂ condensation pressure. Both cycle efficiencies reach a maximum when p_b is increased to the CO₂ condensation pressure, at which point the need for CO₂ compression before its condensation is eliminated, and thus the system changes to the OXYF configuration, which has a lower specific power output, but is more efficient and simpler.

The turbine gas outlet temperature (TOT), increases as p_b is increased, but it remains below 701°C for $p_b < 7.1$ bar due to our choice of the relatively low TIT of 900°C . With this lower temperature of the recuperator REP inlet hot stream (10) temperature, the heat exchanger becomes more conventional, with a much lower price and much higher commercial availability.

5. COMPARISON BETWEEN THE OXYF-COMP AND THE OXYF WITHOUT TURBINE BLADE COOLING

Choosing a TIT value of 900°C to eliminate the need for turbine blade cooling, and to generate the same net power output W_{net} of 20 MW, a comparison was made between the OXYF-COMP and the OXYF systems. Table 3 summarizes the cycle performance.

1) Specific power output: the OXYF-COMP has a higher specific power output

In the OXYF-COMP system, the lower turbine backpressure p_b leads to much higher turbine work output and specific power output w than those in the OXYF: the specific power output of 331 kJ/kg in OXYF-COMP system is 68% higher than the 197 kJ/kg in the OXYF system. 24% of the turbine power output W_{GT} in the OXYF-COMP is consumed by the CO_2 compressors C2 while only 1% of W_{GT} is consumed by the CO_2 compressors C3 in the OXYF.

2) The efficiencies η_e and θ are higher for OXYF than for OXYF-COMP

In the OXYF system, the higher turbine backpressure with a higher turbine exhaust temperature makes more heat available for recuperation, this reducing the fuel (natural gas) demand and the specific power output drops too, but the effect of fuel demand drop dominates. As a result, the OXYF has a thermal efficiency η_e higher by 14.5% than that of the OXYF-COMP.

3) The OXYF system needs/accommodates a higher cooling LNG mass flow rate.

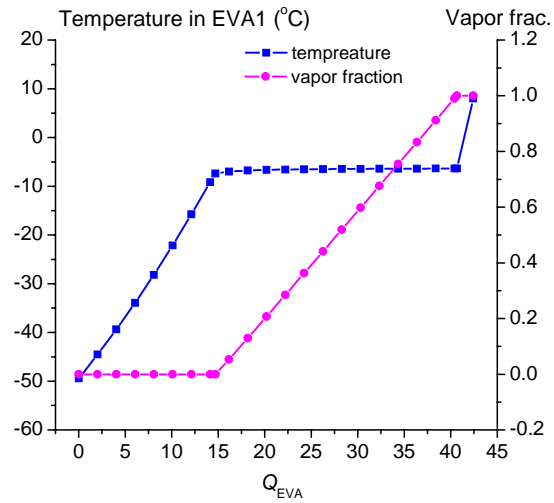


Fig 14 The temperature profile of the produced refrigeration in EVA1 in the OXYF system

Because of the low specific power output in the OXYF system, generation of the same amount electricity (the power generation capacity is fixed in this comparison at 20MW), the OXYF system requires a higher working fluid mass flow rate than that in the OXYF-COMP system, and thus correspondingly a larger LNG mass flow rate is needed (or accommodated, considering the objective of LNG evaporation for ultimate distribution by he terminal) for the cycle heat rejection process. As a result, the OXYF system also produces more cooling from the evaporation of the working fluid and the cooling/evaporating LNG. The produced cooling temperature profile in EVA1 in OXYF is shown in Fig. 14. The refrigeration capacity in EVA1 is about 42.4MW, out of which more than 95% (40.6MW) is produced at temperatures between -50°C to -6°C . and the LNG heating in EVA2 can add 14.5MW cooling capacity in a temperature region of -35°C to 8°C . This information also allows matching of the produced refrigeration with potential commercial need for it.

The exergy efficiency ε , which takes into

accounts both power generation and refrigeration production as commercially-useful outputs, is 6.7% higher in the OXYF than in the OXYF-COMP.

Table 3. Cycle performance summary
Specific exergy of fuel, $e_f = 50.95$ MJ/kg; natural gas LHV = 49.2 MJ/kg.

| | OXYF-COMP | OXYF |
|--|-----------|--------|
| Net power output, W_{net} [MW] | 20 | 20 |
| Turbine blade cooling | no | no |
| CO ₂ compressor intercooling | yes | no |
| CO ₂ condensation pressure [bar] | 7/60* | 7/60* |
| Turbine backpressure p_b [bar] | 1.1 | 7.1 |
| Combustor outlet temperature and pressure [°C/bar] | 900/28 | 900/28 |
| Gas turbine outlet temperature [°C] | 474 | 700 |
| LNG mass flow rate m_{LNG} [kg/s] | 61.93 | 95.54 |
| Natural gas mass flow rate m_f [kg/s] | 0.788 | 0.689 |
| Main working fluid mass flow rate [kg/s] | 60.364 | 101.61 |
| Turbine work output W_{GT} [MW] | 34.151 | 26.535 |
| Power consumption in ASU [MW] | 2.671 | 2.338 |
| Power consumption by CO ₂ pump P1 [MW] | 0.159 | 0.269 |
| Power consumption by air/O ₂ compressor C ₁ [MW] | 1.056 | 0.924 |
| Power consumption by CO ₂ compressor C2 [MW] | 7.915 | --- |
| Power consumption by CO ₂ compressor C3 [MW] | 0.282 | 0.264 |
| Power consumed by LNG pump P2 [MW] | 1.236 | 1.906 |
| | | |
| Heat duty of the recuperator REP [MW] | 27.563 | 74.174 |
| Heat duty of the heat exchanger HEX1 [MW] | 7.844 | 9.746 |
| Heat duty of the heat exchanger HEX2 [MW] | --- | --- |
| Heat duty of the heat exchanger HEX3 [MW] | 1.030 | 0.896 |
| Heat duty of the condenser CON [MW] | 31.116 | 44.939 |
| Cooling capacity of the evaporator EVA1 [MW] | 25.251 | 42.423 |
| Cooling capacity of the evaporator EVA2 [MW] | 1.369 | 14.524 |
| | | |
| Specific power output w [kJ/kg] | 331 | 197 |
| Refrigeration output, Q_C [MW] | 26.62 | 56.95 |
| Refrigeration exergy, E_c [MW] | 4.1 | 8.963 |
| Ratio of power/cooling energy, R | 4.88 | 2.23 |
| CO ₂ recovery ratio, R_{CO_2} [%] | 99.8 | 98.6 |
| CO ₂ emission, [g/kWh] | 0.72 | 4.86 |
| Thermal efficiency, η_e [%] | 51.6 | 59.1 |
| Exergy efficiency, ε [%] | 37.3 | 39.8 |

* 7 bar is the condensation pressure for the main working fluid in the condenser; 60 bar is the condensation pressure for a small fraction of the working fluid in HEX3.

4) Preliminary economic analysis: the OXYF system has a shorter payback period

period (years) which is assumed to be equal to the system life.

The preliminary economic analysis was based on the following assumptions.

- The CO₂ credit price is assumed as 250 CNY (Chinese Yuan) per ton, which is about 25 EUR/ton.
- The electricity price is 0.45 CNY/kWh (0.045 EUR/kWh).
- The price of natural gas from LNG is 1.5 CNY/Nm³ (0.15 EUR/Nm³) for power generation in China.
- The cold energy of LNG is free, and we need not pay for it.
- The annual running time is 7000 hours per year, and the plant life is 20 years. The construction period is 2 years.
- The interest rate is 8%.
- 50% of total investment cost is an interest-bearing loan, and the loan

Balance of plant (BOP) consists of the remaining systems, components, and structures that comprise a complete power plant or energy system that are not included in the prime mover [29]. As the systems are more complex than the conventional power generation system, here we assumed that the BOP account for 20% of the known component cost of the system.

The term O&M is the cost of operating and maintenance, assumed to be 4% of the first cost of the system [30]. Taxes and insurance are not considered in this preliminary evaluation.

The results of the investment of the two systems are listed in Table 4.

Table 4 Investment cost of the two systems

| Items | OXYF | OXYF-COMP |
|--|--------|-----------|
| Air separation unit (10 ³ CNY) | 31600 | 36200 |
| Oxygen compressor (10 ³ CNY) | 3600 | 4000 |
| Gas turbine (10 ³ CNY) | 58000 | 68000 |
| Recuperator (10 ³ CNY) | 20000 | 5000 |
| CO ₂ condenser (10 ³ CNY) | 2500 | 1700 |
| Exhaust gas compressors (10 ³ CNY) | 2600 | 2800 |
| LNG pump (10 ³ CNY) | 2500 | 2000 |
| Low temperature heat exchangers (10 ³ CNY) | 1000 | 800 |
| Second CO ₂ condenser (10 ³ CNY) | 500 | 500 |
| CO ₂ compressor(10 ³ CNY) | -- | 10000 |
| LNG evaporator with sea water (10 ³ CNY) | 3000 | 1800 |
| BOP (10 ³ CNY) | 25060 | 26560 |
| Total plant cost (10 ³ CNY) | 150360 | 159360 |
| Specific cost (CNY/kWe) | 7518 | 7968 |

From Table 4 we can find that the investment cost for the OXYF system is about CNY 7,520/kWe (~\$1,000/kWe), which is 5.6% lower than that for the OXYF-COMP system. These costs are lower than those for power system that include CO₂ separation. Table 5 presents the economic analysis results. The payback

period is calculated with the consideration of interest rate and the 2 years construction period. The cost of electricity in the operation period is calculated as:

$$COE = \frac{\beta C_i + C_m + C_f - C_{CO_2}}{H \cdot W_{net}} \quad (4)$$

C_i is the total plant investment, C_m is the annual the O&M cost, C_f is the annual fuel

cost, and C_{CO_2} is the annual CO₂ credit. The refrigeration profit should be taken into account there is a market for the produced refrigeration. H is the annual operation hours. β is a function of interest rate and the

plant operation life n :

$$\beta = i/[1 - (1 + i)^{-n}] \quad (5)$$

With $n = 20$, and $i = 8\%$, $\beta = 0.1019$.

Table 5 Economic analysis results

| | OXYF | OXYF-COMP |
|---|--------|-----------|
| Annual operation hours | 7,000 | 7,000 |
| Electricity output (million kWh/yr) | 140 | 140 |
| CO ₂ recovery (tons/yr) | 45,360 | 54,583 |
| Natural gas consumption (million Nm ³ /yr) | 24.3 | 27.7 |
| LNG evaporation (million tons/yr) | 2.4 | 1.5 |
| Investment cost (million CNY) | 150.36 | 159.36 |
| Construction interest (million CNY) | 12.51 | 13.26 |
| Total plant investment C_i (million CNY) | 162.87 | 172.62 |
| Income from produced electricity (million CNY/yr) | 63.0 | 63.0 |
| CO ₂ credit C_{CO_2} (million CNY/yr) | 11.34 | 13.65 |
| Cost of fuel C_f (million CNY/yr) | 36.5 | 41.6 |
| O&M C_m (million CNY/yr) | 6.01 | 6.37 |
| Payback period (years) | 8.84 | 10.53 |
| Cost of electricity COE (CNY/kWh) | 0.341 | 0.371 |

The above estimation is based on the assumption that there is no market for the refrigeration. If the refrigeration can also be sold, the payback time will be shortened remarkably by 2-3 years.

The two systems are economically competitive even in comparison with conventional power generation systems which do not have CO₂ recovery and LNG coldness use, having a payback period that is shorter than that of conventional plants, and are thus considered to be feasible and attractive for Chinese LNG stations.

5) Both systems can accomplish high CO₂ capture

The combustion-generated CO₂ recovery ratios are 99.8% and 98.6% for OXYF-COMP and OXYF system, respectively. The recovered CO₂ stream is in the liquid state, and is a mixture of 88% CO₂, 2% O₂, 4% N₂ and 6% Ar by volume. Further purification might be required to remove some components prior to transportation and storage, and would add to

the overall cost [31].

6. CONCLUDING REMARKS

Two power system configurations with LNG cryogenic exergy utilization and CO₂ capture are proposed, simulated and compared. It is found that the OXYF system has higher power generation efficiency, and the OXYF-COMP system has high specific power output. Both systems were found to have high thermal performance and low environment impact.

The influence of the turbine inlet temperature TIT , the turbine blade cooling, and the turbine backpressure were investigated.

It was decided to drop the turbine inlet temperature TIT from 1240°C to 900° to eliminate the need for turbine blade cooling and for advanced gas turbines with the associated technology difficulties and cost. Reduction of the TIT also lowers the turbine exhaust temperature TOT , thus avoiding the technological difficulties and high cost of the high temperature recuperator.

The difference between the two systems is the turbine back pressure. Turbine blade cooling has a higher detrimental effect on the efficiency of the OXYF system that has a higher turbine backpressure and exit temperature, because the working fluid exhausts at the turbine exit is at a higher temperature, and therefore most of the expansion passage in the turbine needs to be cooled. In the OXYF-COMP system the passage portion that must be cooled is by the same token smaller. Without blade cooling, the turbine backpressure has only very weak influence on the system efficiency, and, in fact, the system efficiency increases with the increase of the backpressure in the low backpressure region. This makes the OXYF configuration attractive when the turbine blades aren't cooled.

With TIT at 900°C and no turbine blade cooling, the OXYF-COMP system has a specific power output of 330kJ/kg , and a power generation efficiency of 51.7% . The OXYF system has a specific power output of 197 kg/kg , which is lower by 40% compared with that of the OXYF-COMP system, but it is noteworthy that this value is still comparable or even higher than the specific power output of commercial gas turbines with the same TIT value. The OXYF system has a much higher power generation efficiency of 59.1% as the pressure evaluation is by pump work.

Both systems have a high CO_2 capture ratio.

A preliminary economic evaluation has also been performed. The capital investment cost of the economically optimized plant is about $\$1,000/\text{kWe}$ and the payback period is about 8-10 years including the construction period, both better than those of the latest conventional fossil fuel power plants built in China that do not even separate the CO_2 , and the cost of electricity is estimated to be $0.34\text{-}0.37\text{ CNY/kWh}$.

ACKNOWLEDGEMENT

The authors gratefully acknowledge the

support from the Statoil ASA, and the Chinese Natural Science Foundation Project (No. 50520140517). We would also like to express our great appreciation to Messrs. Geir Johan Rortveit, Bengt Olav Neeraas, Jostein Pettersen and Gang Xu for their very valuable comments and discussion.

APPENDIX

Gas Turbine cooling model

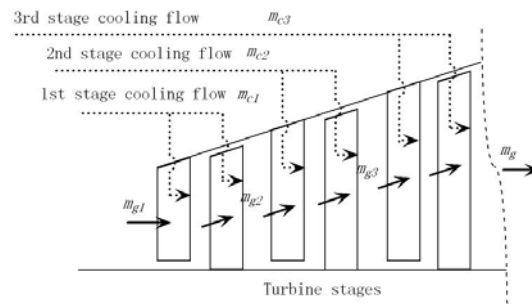


Fig. A1 Schematic diagram of the turbine air cooling model

A discrete (rather than differential field) model was used to analyze the blade cooling and its effects because it is computationally more convenient. As shown in Fig. A1, in such a discrete model we reduced the expansion path into a number of discrete elementary operations, in which the gas expansion process in the turbine includes several mixing processes between the expanding hot gas and the fluid streams added for blade cooling. It considers the turbine stage-by-stage, and estimate the cooling flow necessary for the stator and rotor of each stage. The stator flow is assumed to mix with the main gas flow prior to flow through the turbine, i.e., the mixing happens before the power extraction. The rotor coolant flow is mixed into the main stream at the rotor exit (after the power extraction).

For each cooling step, the required coolant mass flow is calculated using [32-34]:

$$\frac{m_c}{m_g} = \frac{C_{pg}}{C_{pc}} St_g \frac{A_b}{A_g} \frac{1}{\eta_c} \frac{\varepsilon_c}{1-\varepsilon_c} (1-e_f) \quad (A1)$$

where subscripts g and c refer to the main gas stream and the cooling stream, respectively. St_g is main gas Stanton number, A_b is the blade surface area, A_g is the flue gas path cross-sectional area, η_c is the cooling efficiency.

The cooling effectiveness ε_c is defined as:

$$\varepsilon_c = (T_g - T_b) / (T_g - T_c) \quad (A2)$$

For an advanced gas turbine generation, commonly used values for St_g , A_b/A_g and η_c are 0.005, 4 and 0.3 [35]. T_b refers to the turbine blade metal temperature; its typical value is 1100K and is kept constant in the calculation.

Comparing with internal convection cooling, the cooling flow rate requirement is reduced by more than 40% if film cooling is employed. The film cooling effectiveness e_f is adopted in the present study to account for this difference. $e_f=0.47$ for film cooling, and $e_f=0$ in case of simply convective cooling with no film [36].

The pressure loss due to the mixing of the coolant with the gas was set as equal to the ratio between the local coolant mass flow and the corresponding main gas mass flow [36]

$$\Delta p_{mix}(i) = m_c(i) / m_g(i) \quad (A3)$$

For the oxy-fuel systems proposed and analyzed in this study, the coolant for the blade cooling is extracted continuously from the working fluid in the recuperator *REP*, the extracted stream is the recycled CO₂ stream at the state of 200°C/29bar.

The cooled stages are divided based on the expansion profile of OXYF-COMP because of its full expansion. The turbine in OXYF-COMP is divided into 4 stages assuming equal enthalpy drops. Once the mixing point pressures are determined, they are fixed regardless of the variation of the turbine backpressure, which means that in

OXYF, the dividing point of each stage is the same as that in OXYF-COMP. This assumption is based on the fact that they share the same temperature profile in the higher pressure expansion where blade cooling is employed. Starting from the first stage, the turbine cooling model (eqs. (A1-A3)) has been applied to determine the coolant ratio for each stator and rotor, until the working gas reached the allowed metal blade temperature T_b , thus dividing the expansion passage into cooled part and uncooled part. The uncooled part shrinks as the turbine backpressure increases; the turbine in OXYF is almost all the cooled part.

It is noteworthy that in this study we assume that film cooling is used for the blades. If more advanced cooling, such as transpiration blade cooling, would be used, the efficiency loss would be much lower than we calculate here, only a few percent.

REFERENCES

- [1] Karashima N., and Akutsu T., 1982, Development of LNG Cryogenic Power Generation Plant, Proceedings of 17th IECEC, pp. 399-404.
- [2] Angelino G., 1978, The Use of Liquid Natural Gas as Heat Sink for Power Cycles, ASME Journal of Engineering for Power, 100, pp. 169-177.
- [3] Kim C. W., Chang S. D., Ro, S. T., 1995, Analysis of the Power Cycle Utilizing the Cold Energy of LNG, International Journal of Energy Research, 19, pp. 741-749.
- [4] Najjar Y. S. H., Zaamout M. S., 1993, Cryogenic Power Conversion with Regasification of LNG in a Gas Turbine Plant, Energy Convers. Mgmt, 34, pp. 273-280.
- [5] Wong W., 1994, LNG Power Recovery, Proceedings of the Institution of Mechanical Engineers, Part A: Journal of Power and Energy, 208, pp. 1-12.
- [6] Deng S., Jin H., Cai R., Lin R., 2004, Novel Cogeneration Power System with

- Liquefied Natural Gas (LNG) Cryogenic Exergy Utilization, *Energy*, 29: 497-512.
- [7] Krey G., 1980, Utilization of the Cold by LNG Vaporization with Closed-Cycle Gas Turbine, *ASME Journal of Engineering for Power*, 102, pp. 225-230.
- [8] Agazzani A., Massardo A. F., 1999, An Assessment of the Performance of Closed Cycles with and without Heat Rejection at Cryogenic Temperatures, *ASME Journal of Engineering for Gas Turbines and Power*, 121, pp. 458-465.
- [9] Deng S., Jin H., et al, 2001, Novel Gas Turbine Cycle with Integration of CO₂ Recovery and LNG Cryogenic Exergy Utilization, *Proceedings of ASME IMECE 2001*.
- [10] Chiesa P., 1997, LNG Receiving Terminal Associated with Gas Cycle Power Plants, *ASME paper 97-GT-441*.
- [11] Desideri U., and Belli C., 2000, Assessment of LNG Regasification Systems with Cogeneration, *Proceedings of TurboExpo 2000*, Munich, Germany, 2000-GT-0165.
- [12] Kim T. S., and Ro S. T., 2000, Power Augmentation of Combined Cycle Power Plants Using Cold Energy of Liquefied Natural Gas, *Energy*, 25, pp. 841-856.
- [13] Velautham S., Ito T., Takata Y., 2001, Zero-Emission Combined Power Cycle Using LNG Cold, *JSME International Journal, Series B. Fluids and Thermal Engineering*, 44, pp. 668-674.
- [14] Riemer P., 1996, Greenhouse Gas Mitigation Technologies, an Overview of the CO₂ Capture, Storage and Future Activities of the IEA Greenhouse Gas R&D Program, *Energy Conversion and Management*, 37, pp. 665-670.
- [15] Haugen H. A., Eide L. I., 1996, CO₂ Capture and Disposal: the Realism of Large Scale Scenarios, *Energy Convers. Mgmt*, 37, pp. 1061-1066.
- [16] Jericha H., Gottlich E., Sanz W. and Heitmeir F., Design Optimization of the Graz Cycle Prototype Plant, *ASME Journal of Engineering for Gas Turbines and Power*, Vol. 126: 733-740, 2004.
- [17] Anderson R., Brandt H., Doyle S., Pronske K., Viteri F., Power Generation with 100% Carbon Capture and Sequestration, 2nd Annual Conference on Carbon Sequestration, Alexandria, VA, 2003.
- [18] Marin O., Bourhis Y., Perrin N., Zanno P. D., Viteri F., Anderson R., High Efficiency, Zero Emission Power Generation Based on a High-Temperature Steam Cycle, 28th International Technical Conference on Coal Utilization & Fuel Systems, Clearwater, FL, USA, 2003.
- [19] Mathieu P. and Nihart R., Zero-Emission MATIANT Cycle, *Journal of Engineering for Gas Turbines and Power*, Vol. 121: 116-120, 1999.
- [20] Mathieu P. and Nihart R., Sensitivity Analysis of the MATIANT Cycle, *Energy Conversion and Management*, Vol. 40: 1687-1700, 1999.
- [21] Zhang N. and Lior N., A Novel Near-Zero CO₂ Emission Thermal Cycle with LNG Cryogenic Exergy Utilization, *Energy*, 31: 1666-1679, 2006.
- [22] Zhang N. and Lior N., Proposal and Analysis of a Novel Zero CO₂ Emission Cycle with Liquid Natural Gas Cryogenic Exergy Utilization, *Journal of Engineering for Gas Turbine and Power*, 128: 81-91, 2006.
- [23] Ishida M., and Jin H., CO₂ Recovery in a Novel Power Plant System with Chemical-Looping Combustion, *J. of Energy Conv. and Manag.*, Vol. 38, No. 19, 187-192 1997.
- [24] Ishida M., and Jin H., A New Advanced Power-generation System Using Chemical-looping Combustion, *Energy - The International Journal*, 19, 415-422, 1994.
- [25] Griffin T., Sundkvist S. G., Asen K. and Bruun T., Advanced Zero Emissions Gas Turbine Power Plant, *ASME Journal of Engineering for Gas Turbines and Power*, Vol. 27: 81-85, 2005.

- [26] Kvamsdal H. M., Jordal K., Bolland O., A Quantitative Comparison of Gas Turbine Cycles with CO₂ Capture, *Energy*, 32:10-24, 2007.
- [27] Aspen Plus[®], Aspen Technology, Inc., Version 11.1, <http://www.aspentech.com/>.
- [28] Lior N., Zhang N., Energy, Exergy, and Second Law Performance Criteria, *Energy – The International Journal*, 32: 281-296, 2007.
- [29] Larson E. D., Ren T, Synthetic fuel production by indirect coal liquefaction, *Energy for Sustainable Development*, Vol. VII No. 4, 2003.
- [30] Kreutz T., Williams R., Consonni S., Chiesa P., Co-production of Hydrogen, Electricity and CO₂ from Coal with Commercially Ready Technology. Part B: Economic analysis, *Hydrogen energy*, 30: 769-784, 2005.
- [31] Davison J., Performance and Cost of Power Plants with Capture and Storage of CO₂, *Energy* 2007; 32: 1163-1176.
- [32] Stecco S., Facchini B., A Computer Model for Cooled Expansion in Gas Turbines, *Proc. The ASME Cogen-Turbo Symposium, Nice, France, 1989*.
- [33] Abdallah H., Harvey S., Thermodynamic analysis of chemically recuperated gas turbines, *Int. J. Therm. Sci*, 40, 372-384, 2001.
- [34] Jordal K., Bolland O., Klang A., Aspects of Cooled Gas Turbine Modeling for the Semi-closed O₂/CO₂ Cycle with CO₂ Capture, *ASME J. Engineering for Gas Turbines and Power*, 126, 507-515, 2004.
- [35] Elmasri M. A., On Thermodynamics of Gas Turbine Cycles: Part 2 – A Model for Expansion in Cooled Turbines, *ASME J. Engineering for Gas Turbines and power*, 108, 151-159, 1986.
- [36] Fiaschi D., Lombardi L., Cellular Thermodynamic Model for Gas Turbine Blade Cooling, *Proceeding of ECOS2001*, 2001.

